

NUMERICAL INVESTIGATION OF THE COUNTER-INTUITIVE BEHAVIOR OF MACH DISK MOVEMENT IN UNDEREXPANDED GAS-PARTICLE JETS

O. Ejtehad¹, A. Rahimi² and R.S. Myong^{*2,3}

¹Supercomputing Modeling and Simulation Center, Korea Institute of Science and Technology Information

²Graduate School of Mechanical and Aerospace Engineering, Gyeongsang National University

³Dept. of Aerospace and Software Engineering & ReCAPT, Gyeongsang National University

과소팽창 가스-입자 제트의 MACH 디스크의 비직관적 거동 수치연구

오미드 에즈태하디,¹ 아민 라히미,² 명 노 신^{*2,3}

¹한국과학기술정보연구원 가상설계센터

²경상대학교 대학원 기계항공공학부

³경상대학교 항공우주및SW공학전공 및 항공기부품기술연구소

An important feature in the problem of underexpanded jets is the prediction of the location of the Mach disk. In the current study, a discontinuous Galerkin solver is applied to the two-fluid system of equation of the dusty gas flow for predicting the location of the Mach disk when solid particles are added. It has been known that for small particle diameters the increase of particulate loading leads to an upstream movement of the Mach disk. In this study, it is proposed that the effective parameter controlling the Mach disk movement is the Stokes number. The validity of this proposition is investigated by a series of numerical simulations. The results indicate that for low Stokes number flows there is a downstream movement, while for high Stokes number flows there is an upstream movement. Furthermore, it is shown that for more accurate predictions in comparison with experimental results it is necessary to assign an equivalent mixture speed at the inlet.

Key Words : particle-laden underexpanded jets, Mach disk location, discontinuous Galerkin method, Eulerian-Eulerian model

1. Introduction

Supersonic jets issuing from underexpanded nozzles are observed in various practical engineering applications ranging from plumes of aircraft and rockets to supersonic combustors. On the other hand, this type of flows is a suitable benchmark problem for studying the complex wave patterns due to interaction of shock waves with particles [1]. An essential parameter pertinent to the

problem of the underexpanded jet is the prediction of the location of the Mach disk. From a physics point of view, understanding this feature is a key in the fundamentals of gas dynamics. Moreover, this property is essential in predicting the structure of the plume of the nozzle (an important system design requirement). Therefore, such studies can be crucial in various engineering applications based on the concept of jet under-expansion. Examples include jet propulsions, natural gas pipeline blowdowns, and radio jets. This parameter has long been investigated experimentally [2-7] and numerically [8-11]. A comprehensive review regarding the Mach disk position, diameter, and apparition of free underexpanded jets in the quiescent medium can be found in the paper by Franquet *et al.* [12]. The schematic of the problem defined as a

Received: October 15, 2018, Revised: March 16, 2019,

Accepted: March 16, 2019.

* Corresponding author, E-mail: myong@gnu.ac.kr

DOI <http://dx.doi.org/10.6112/kscfe.2019.24.1.019>

© KSCFE 2019

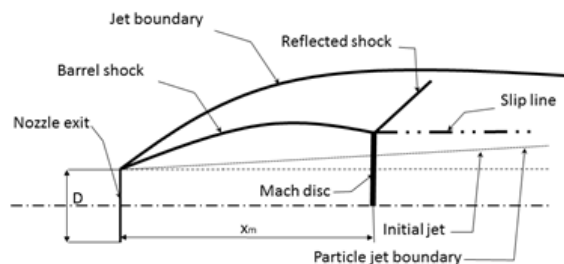


Fig. 1 Schematic of the under-expanded jet problem

supersonic jet expanding from a high-pressure chamber into a low-pressure ambient is illustrated in Fig. 1.

In some applications such as in solid propellant rocket boosters, injection of powder fuel into the combustion chamber or volcanic eruptions, the presence of particles can subsequently change the dynamics of the flow. Even though the gas-only flow of the underexpanded jets has been studied from different perspectives in an abundant number of works, the particle-laden underexpanded jets are addressed only in a limited number of researches. Sommerfeld [13] studied the effect of particle diameter and ambient pressure on the structure of the underexpanded jets with the use of a discrete particle methods and a piecewise linear method. In another work, Sommerfeld [14] applied Lagrangian formulation on structured grids to investigate supersonic two-phase gas-particle flows. Hayashi *et al.* [15] applied an Eulerian formulation to investigate the dynamics between a gas phase and a solid phase in terms of the size and loading ratio of solid particles. Ishii *et al.* [16] comprehensively investigated the underexpanded supersonic free-jet flows and supersonic flows around a truncated cylinder of gas-particle mixtures using an Eulerian-Lagrangian framework. In the numerical dusty gas flows studies mentioned above, a downstream movement of the Mach disk location was predicted which is in contradiction with the early experimental results of [2,17] and more recent experiment of [18]. In the latter, a combined experimental and numerical study was conducted by which a correlation for the inlet velocity of the gas phase was established.

The current paper aims to expand upon the counter-intuitive trend (downstream vs. upstream movement of the Mach disk) by using a high-order accurate numerical approach, i.e., discontinuous Galerkin method. Previous studies only considered the effect of variation of particles diameter on the behavior of the underexpanded jets. However, the parameter that explains the interaction of the dust and gas phase is the Stokes number. We

hypothesize that besides particle diameter all the other parameters present in the Stokes number relation, including dust particle microscopic density, gas viscosity and reference values of velocity and characteristic length would affect the movement of the Mach stem. To the best knowledge of the authors, this is the first time that details of such phenomena are being investigated. Here, after verification and validation of the numerical method and demonstration of the counter-intuitive behavior for different particle diameters, we analyze the role of the Stokes number independently for various particulate loadings.

2. Mathematical Modeling and Numerical Procedure

The high computational cost of the Lagrangian methods especially when coupling of the solid and gas phases on an unstructured grid is required, motivated using an Eulerian framework in this work. Some assumptions, conventional in the pioneering and previous literature regarding the two-fluid model are introduced to simplify the computations. In majority of the two-fluid models which considered dusty gas flows, the gas phase is considered as compressible which follows the perfect-gas law and the solid phase is considered as incompressible. The inter-particle collisions are neglected (thus no pressure term in the solid phase conservation law) and the particles are assumed to be uniform sized spheres with a constant diameter and microscopic density. The specific heat of the particles material is constant, and the temperature is uniform within each particle. Moreover, particles are considered as inert and the thermal and Brownian motion of particles are neglected. Furthermore, the gravitational and buoyant forces, the turbulence effects and the effect of particles' wake are considered to be negligible. In this model, the number density of the particles should be large enough not to violate the continuum assumption.

While some of the assumptions introduced above are due to inherent characteristics of the model which cannot be recast, some of the others that have been used in the previous literature can be modified in order to provide solutions closer to reality and specific to the investigated problem. For example, the effect of gravity (which finds importance in problems such as volcanic eruptions) can be quickly taken into account by additional source terms without disturbing any fundamental assumptions [19-21]. The viscous effects in the gas phase can be considered by addition of viscous fluxes in the generic model. The models for inter-particle collisions has been also proposed and implemented [22-24]. Furthermore, kinetic theory

approaches have been considered for continuum modeling of the dispersed phase [25].

2.1. Governing equation

Under the above conditions, the conservation law (with taking viscous effects into account) can be written as follows:

For the gas phase,

$$\partial_t \mathbf{U}_g + \nabla \cdot \mathbf{F}_g = \mathbf{S} \quad (1)$$

$$\mathbf{U}_g = \begin{bmatrix} \alpha_g \rho_g \\ \alpha_g \rho_g \mathbf{u}_g \\ \alpha_g \rho_g E_g \end{bmatrix}, \quad \mathbf{F}_g = \begin{bmatrix} \alpha_g \rho_g \mathbf{u}_g \\ \alpha_g \rho_g \mathbf{u}_g \mathbf{u}_g + p \mathbf{I} + \mathbf{\Pi}_g \\ (\alpha_g \rho_g E_g + p) \mathbf{u}_g + \mathbf{\Pi}_g \cdot \mathbf{u}_g + \mathbf{Q}_g \end{bmatrix}, \quad \mathbf{S} = \begin{bmatrix} 0 \\ D_{g,s} (\mathbf{u}_s - \mathbf{u}_g) \\ D_{g,s} (\mathbf{u}_s - \mathbf{u}_g) \mathbf{u}_s + Q_{g,s} (T_s - T_g) \end{bmatrix} \quad (2)$$

Moreover, for the solid phase:

$$\partial_t \mathbf{U}_s + \nabla \cdot \mathbf{F}_s = -\mathbf{S} \quad (3)$$

$$\mathbf{U}_s = \begin{bmatrix} \alpha_s \rho_s \\ \alpha_s \rho_s \mathbf{u}_s \\ \alpha_s \rho_s E_s \end{bmatrix}, \quad \mathbf{F}_s = \begin{bmatrix} \alpha_s \rho_s \mathbf{u}_s \\ \alpha_s \rho_s \mathbf{u}_s \mathbf{u}_s + \mathbf{\Pi}_s \\ (\alpha_s \rho_s E_s) \mathbf{u}_s + \mathbf{\Pi}_s \cdot \mathbf{u}_s + \mathbf{Q}_s \end{bmatrix} \quad (4)$$

Here, \mathbf{U} , \mathbf{F} , and \mathbf{S} are the vectors of conservative variables, fluxes, and source terms, respectively. The variables t , α , ρ , \mathbf{u} , E , p , T , $\mathbf{\Pi}$, and \mathbf{Q} represent time, volume fraction, density, velocity vector, total energy, pressure, temperature, stress tensor and heat flux vector. In the above equations, the dust microscopic density ρ_s is assumed to be constant. Further, $D_{g,s}$ and Q_g denote inter-phase drag and heat flux, respectively, which can be calculated according to the following relations:

$$D_{g,s} = \frac{3}{4} C_D \frac{\alpha_s \rho_g}{d} |u_g - u_s| \quad (5)$$

$$Q_g = \frac{6N\kappa_g}{d^2} \alpha (T_g - T_s) \quad (6)$$

where,

$$C_D = \begin{cases} \frac{24}{Re_d} (1 + 0.15 Re_d^{0.687}), & \text{if } Re_d \leq 1000 \\ 0.44, & \text{if } Re_d > 1000 \end{cases} \quad (7)$$

$$Nu = 2 + 0.65 Re_d^{\frac{1}{2}} Pr^{\frac{1}{3}}, Pr = \frac{c_p \mu_g}{\kappa_g} \quad (8)$$

In the above relations, d is the particle diameter, Re_d is the Reynolds number based on the particle diameter and relative velocity of the particle to the gas. Furthermore, μ_g , κ_g and c_p represent the viscosity, thermal conductivity, and specific heat capacity at constant pressure of the gas, respectively.

The above system of equations were written in a general form and can be easily rewritten for one to three-dimensional flows. However, a particular case is the three-dimensional flows with axial symmetry. A two-dimensional formulation using the two space variables (x , r) can be achieved by rewriting the equations in cylindrical coordinates (x , r , θ). Extension of this system of equations for viscous flows and for the dust phase is trivial.

$$\frac{\partial}{\partial t} (\mathbf{U}_g) + \frac{\partial}{\partial x} \mathbf{F}_g(\mathbf{U}_g) + \frac{\partial}{\partial r} \mathbf{G}_g(\mathbf{U}_g) = \mathbf{S}_1 + \mathbf{S}_2 \quad (9)$$

$$\mathbf{U}_g = \begin{bmatrix} \alpha_g \rho_g \\ \alpha_g \rho_g u_g \\ \alpha_g \rho_g v_g \\ \alpha_g \rho_g E_g \end{bmatrix}, \quad \mathbf{F}_g = \begin{bmatrix} \alpha_g \rho_g u_g \\ \alpha_g \rho_g u_g^2 + p \\ \alpha_g \rho_g u_g v_g \\ (\alpha_g \rho_g E_g + p) u_g \end{bmatrix}, \quad \mathbf{G}_g = \begin{bmatrix} \alpha_g \rho_g v_g \\ \alpha_g \rho_g u_g v_g \\ \alpha_g \rho_g v_g^2 + p \\ (\alpha_g \rho_g E_g + p) v_g \end{bmatrix}, \quad \mathbf{S}_1 = \begin{bmatrix} 0 \\ D_{g,s} (u_s - u_g) \\ D_{g,s} (v_s - v_g) \\ D_{g,s} ((u_s - u_g) u_s + (v_s - v_g) v_s) + Q_{g,s} (T_s - T_g) \end{bmatrix}, \quad \mathbf{S}_2 = \frac{1}{r} \begin{bmatrix} \alpha_g \rho_g v_g \\ \alpha_g \rho_g u_g v_g \\ \alpha_g \rho_g v_g^2 \\ (\alpha_g \rho_g E_g + p) v_g \end{bmatrix} \quad (10)$$

In the above relations, x and r are the axial and radial directions; u and v are the corresponding velocities. \mathbf{F} and \mathbf{G} are the inviscid flux in axial and radial directions. \mathbf{S}_1 and \mathbf{S}_2 are source terms responsible for phase interactions and axisymmetric geometry.

2.2. Discontinuous Galerkin method

For solving the above system of equations, the discontinuous Galerkin method was selected due to the unique features the method suggests. The method was first

introduced by Reed and Hill[26], and further was developed in [27-29]. Recently, the DG method has become a prominent tool for solving the fluid dynamics governing equations in different fields including compressible and incompressible flows, aeroacoustics, magneto-hydrodynamics, and multiphase flows [30].

The mathematical model of interest in the present work can be written in a compact form:

$$\partial_t \mathbf{U} + \nabla \cdot \mathbf{F}_{inv}(\mathbf{U}) + \nabla \cdot \mathbf{F}_{vis}(\mathbf{U}, \nabla \mathbf{U}) = \mathcal{S}(\mathbf{U}) \quad (11)$$

$$[(t, \Omega) | t \in (0, \infty), \Omega \subset R]$$

where Ω denotes a bounded domain, and \mathbf{U} , \mathbf{F}_{inv} , \mathbf{F}_{vis} , \mathcal{S} are conservative variables vector, inviscid flux vector, viscous flux vector, and source terms vector, respectively. The solution domain can be decomposed by a group of non-overlapping elements, $\Omega = \Omega_1 \cup \Omega_2 \cup \dots \cup \Omega_n$, in which n is the number of elements. The partial differential equation of (11) can not allow for solutions with discontinuities. By multiplying a weighting function ϕ into the conservative laws (11) and integrating over the control volume for each element, the following formulation can be derived:

$$\int_{\Omega_k} [\partial_t \mathbf{U} \phi(x) + \nabla \cdot \mathbf{F}_{inv}(\mathbf{U}) \phi(x) + \nabla \cdot \mathbf{F}_{vis}(\mathbf{U}) \phi(x) - \mathcal{S}(\mathbf{U}) \phi(x)] d\Omega = 0 \quad (12)$$

In the present work, PDK polynomials are selected as basis functions and a collapse coordinate transformation is used to transfer the triangular meshes in the physical domain to the standard square elements [1].

As can be seen in (11) and (12), when the solution of viscous flows is of interest, an approach for estimation of the derivatives of the conserved variable which appear in the viscous flux terms should be applied. These first-order derivatives will change into second-order derivatives when the viscous fluxes are evaluated. These terms cannot be accommodated directly in a weak variational formulation using a discontinuous space function. One possible approach is the addition of a set of separate equations to regard the gradient of the conservative variables as an auxiliary set of unknowns, as proposed by Bassi and Rebay [31]. In this work, auxiliary variable \mathbf{A} is chosen to be the derivatives of the conserved variables \mathbf{U} , i.e., $\mathbf{A} = \nabla \mathbf{U}$. This approach is known as mixed DG formulation and will result in the following coupled system:

$$\mathbf{A} - \nabla \mathbf{U} = 0 \quad (13)$$

$$\partial_t \mathbf{U} + \nabla \cdot \mathbf{F}_{inv}(\mathbf{U}) + \nabla \cdot \mathbf{F}_{vis}(\mathbf{U}, \nabla \mathbf{U}) = \mathcal{S}(\mathbf{U})$$

Then the solution of the primary and auxiliary variables can be approximated as,

$$\mathbf{U}_h = \sum_i^P U_i(t) \phi_i(x), \mathbf{A}_h = \sum_i^P A_i(t) \phi_i(x) \quad (14)$$

where $U_i(t)$, $A_i(t)$ denotes the local degree of freedom for the auxiliary variable. By multiplying a weighting function ϕ_i into the conservative laws and integrating over the control volume for each element, the following formulation can be derived:

$$\int_{\Omega_k} [\mathbf{A} \phi(x) - \nabla \mathbf{U} \phi(x)] d\Omega = 0 \quad (15)$$

$$\int_{\Omega_k} [\partial_t \mathbf{U} \phi(x) + \nabla \cdot \mathbf{F}_{inv}(\mathbf{U}) \phi(x) + \nabla \cdot \mathbf{F}_{vis}(\mathbf{U}) \phi(x) - \mathcal{S}(\mathbf{U}) \phi(x)] d\Omega = 0 \quad (16)$$

By splitting the integral over Ω_h into series of the integrals over the sub-elements and applying the integration by part as well as divergence theorem to the equations (15) and (16),

$$\int_{\Omega_k} \phi_i(x) \mathbf{A}_h d\Omega_k - \oint_{\partial\Omega_k} \phi_i(x) \mathbf{U}_h \cdot \hat{n} d\sigma + \int_{\Omega_k} \nabla \phi_i(x) \cdot \mathbf{U}_h d\Omega_k = 0 \quad (17)$$

$$\int_{\Omega_k} \partial_t \mathbf{U}_h \phi_i(x) d\Omega_k + \oint_{\partial\Omega_k} \phi_i(x) \mathbf{F}_{inv}(\mathbf{U}_h) \cdot \hat{n} d\sigma - \int_{\Omega_k} \nabla \phi_i(x) \cdot \mathbf{F}_{inv}(\mathbf{U}_h) d\Omega_k + \oint_{\partial\Omega_k} \phi_i(x) \mathbf{F}_{vis}(\mathbf{U}_h) \cdot \hat{n} d\sigma - \int_{\Omega_k} \nabla \phi_i(x) \cdot \mathbf{F}_{vis}(\mathbf{U}_h) d\Omega_k = \int_{\Omega_k} \phi_i(x) \mathcal{S}(\mathbf{U}_h) d\Omega_k \quad (18)$$

Here, \hat{n} is the outward unit normal vector of the element interface and \mathbf{U}_h is the p -exact polynomial approximated solutions of the \mathbf{U} on the discretized domain of Ω_h . The Rusanov (or local Lax-Friedrichs) flux function along with positivity and monotonicity limiters are applied for the shock capturing. The Rusanov flux function is shown to

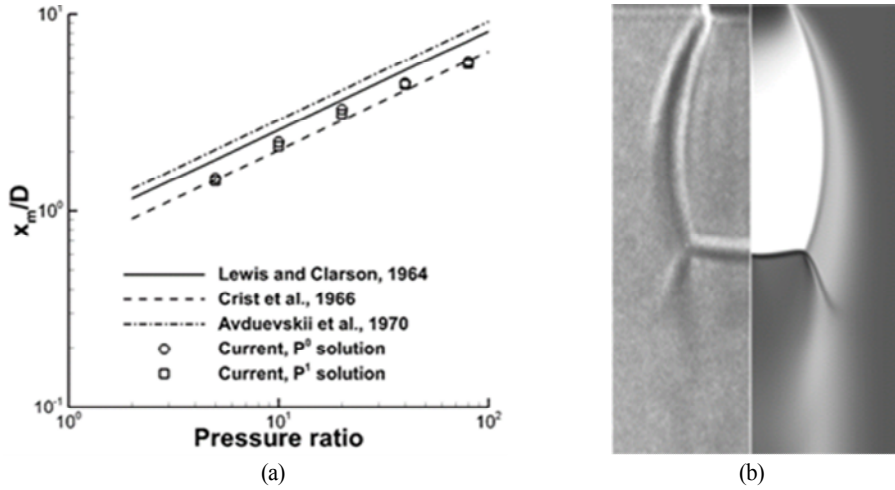


Fig. 2 Validation of results for pure gas

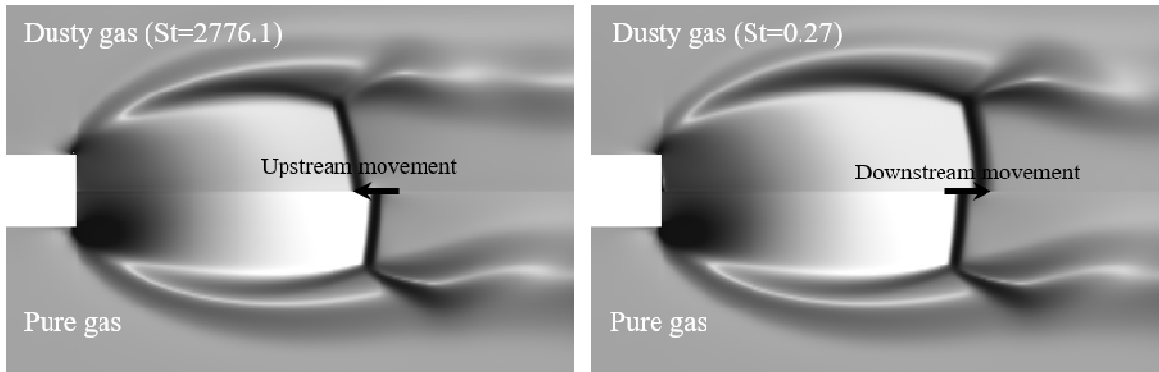


Fig. 3 Effects of addition of dust particles with different diameters on Mach disk location

provide a stable schemes and has been widely used in various DG codes. The process of estimation of surface and volume integrals are analogous to the inviscid system procedure [1]. It should be noted that, for the auxiliary terms (essential in estimation of viscous terms), a central flux splitting scheme is applied.

$$\begin{aligned}
 \mathbf{F}_{vis}(\mathbf{U}_h) &\approx f_{i,vis}(\mathbf{U}_h^-, \mathbf{A}_h^-, \mathbf{U}_h^+, \mathbf{A}_h^+) \\
 &= \frac{1}{2} [\mathbf{F}_{i,vis}(\mathbf{U}_h^-, \mathbf{A}_h^-) + \mathbf{F}_{i,vis}(\mathbf{U}_h^+, \mathbf{A}_h^+)] \\
 \mathbf{U} &\approx f_{i,aux}(\mathbf{U}_h^-, \mathbf{U}_h^+) = \frac{1}{2} [\mathbf{U}_h^-, \mathbf{U}_h^+]
 \end{aligned}
 \tag{19}$$

3. Results and Discussion

The crucial parameter in fluid-particle flows to characterize the response rate of the particles to changes

in fluid motion or to evaluate the kinetic equilibrium of the particles with the carrier gas, is the Stokes number, defined as

$$St = \frac{\tau_V}{t_{ref}} \tag{20}$$

Here t_{ref} is a reference time defined as characteristic length (often nozzle diameter in the literature) divided by the characteristic speed and, τ_V is the momentum (velocity) response time of the particles given by

$$\tau_V = \frac{\rho_s d^2}{18\mu_g} \tag{21}$$

$St \ll 1$ implies that the response time of the particles is much less than the characteristic time of the flow. In

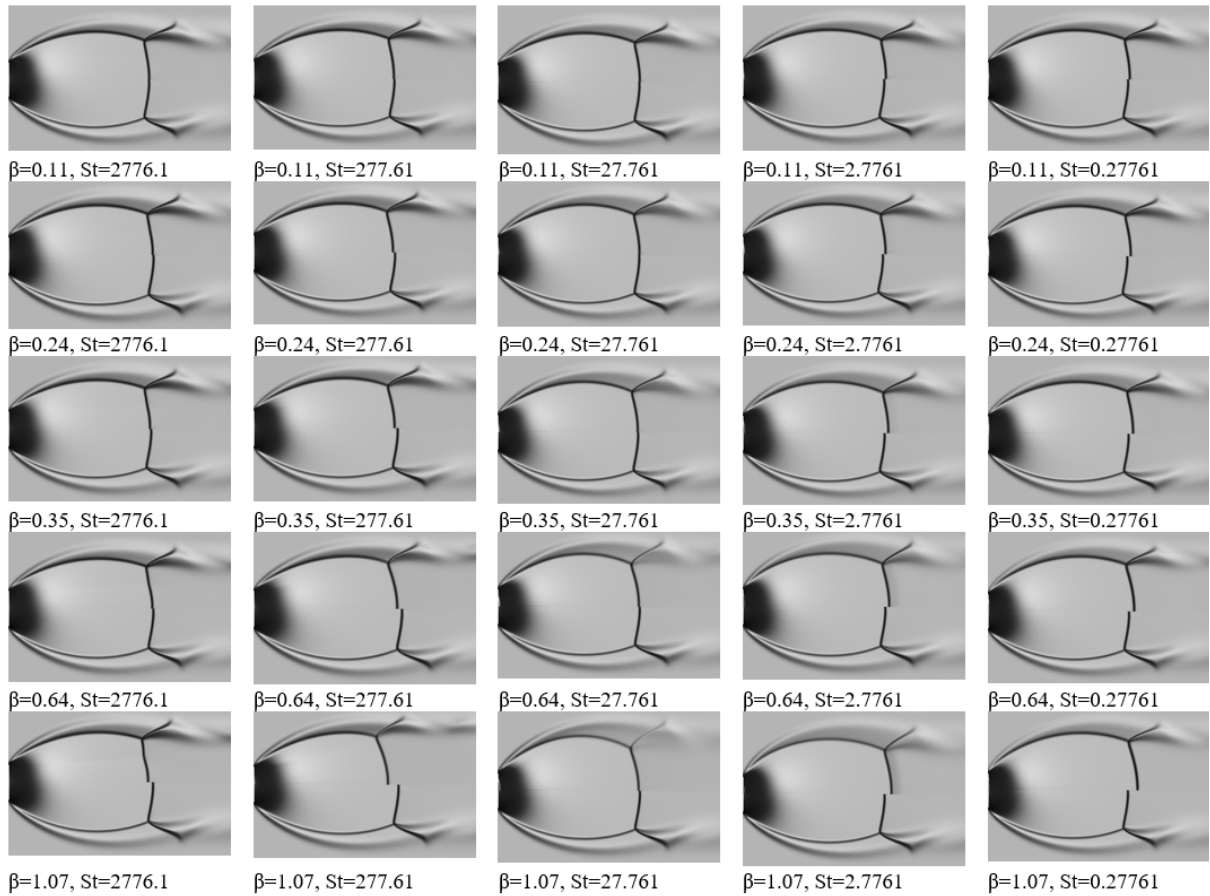


Fig. 4 Effect of variation of particulate loading and Stokes number on Mach contours in the under-expanded jet problem ($p_0/p_\infty = 29.8$)

this case, the particles have enough time to equilibrate with the carrier phase leading to nearly equal velocities. These types of flow can be accurately simulated with a one-way coupled model. On the other extreme, when $St \gg 1$, the response time of the particles is much more than that of the carrier phase. Consequently, particle velocity is little affected by the fluid velocity change. A two-way coupling algorithm should thus take into account the back-influence of the particle phase on the carrier fluid.

3.1. Validation and verification of the results

Prior to numerical investigations, the validity of numerical solutions are examined. The numerical tool has been extensively validated for the inviscid gas flows in [1]. For the purpose of validation of the viscous solver in the problem of underexpanded jet, the location of the Mach disk (in a pure gas) for different pressure ratios

(p_0/p_∞) is compared with the empirical relations of previous experimental studies, as shown in Fig. 2(a). The comparison indicates that the numerical solution can provide predictions close to experiments. It can be seen that when first order polynomials (P^1) are applied the location of the Mach disk is slightly underestimated compared to the second order solution (P^2).

In Fig. 2(b), a comparison of the Mach contour with schlieren image of an experimental test case reported in [18] where $p_0/p_\infty = 29.8$ is provided, which demonstrates a good qualitative agreement in terms of prediction of the geometrical shape of the jet with experimental results. Moreover, a qualitative validation for the case of dusty gas can be found in [1]. Further, for all the simulations, the second-order (P^2) polynomials were applied.

3.2. Counter-intuitive trend in movement of the Mach disk

While all the previous experimental results indicate an

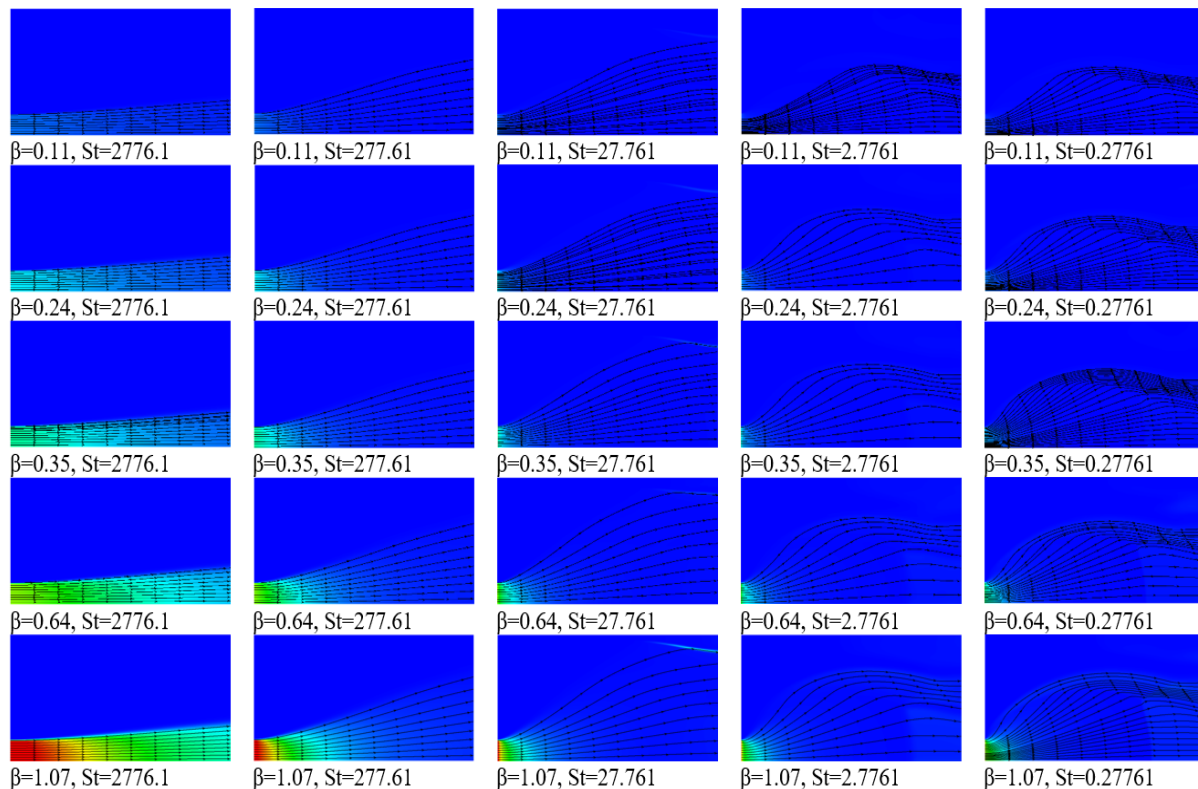


Fig. 5 Effect of variation of particulate loading and Stokes number on density contours and particles streamlines in the under-expanded jet problem ($p_0/p_\infty = 29.8$)

upstream movement of the Mach disk, in some of the numerical reports the trend contradicts the experiments. This counter-intuitive behavior is observed for small-diameter particles. Here, the effect of particle diameter on the movement of the Mach disk is studied for two different particle diameters, i.e., $d = 1 \mu m$ and $d = 100 \mu m$. Glass beads with the macroscopic density of $2500 kg/m^3$ are simulated. The characteristic length (in the Stokes relation) is set equal to 0.01 and air with the viscosity of $1.65 \times 10^{-5} Pa.s$ at 273.15 K is selected as the carrier phase. The corresponding Stokes numbers are 0.27 and 2776 for 1 and 100 micron particles, respectively. As shown in Fig. 3 for smaller particles the Mach disk shows a downstream movement while for larger particles the movement of the Mach disk is upstream-wise compared to the pure gas case. It is interesting to note that the experimental results of [18] indicate an upstream motion for particles with a diameter of 45 μm .

3.3. Effects of Stokes number with characteristic length

According to equations (20) and (21), the Stokes

number can be assigned by variation of different parameters including particle diameter, the density of the particle phase, the viscosity of the carrier phase or characteristic time of the flow. Here Stokes number is artificially assigned by multiplying a constant coefficient to the source terms so that only coupling effects are investigated. It has been demonstrated through experiments of Sommerfeld [18] that the Mach disk location moves towards the jet exit plane by the increase of the particulate loadings. However, in Fig. 3 a counter-intuitive behavior is observed in case of low Stokes number flows. Fig. 4 demonstrates a more detailed analysis on the role of Stokes and particulate loading (β defined as the mass of particles per unit volume of the carrier phase) on the location of the Mach disk. Here the Mach contours of the dusty gas flow are compared with the pure gas case. The Mach disk displacement trend changes from an upstream movement to a downstream movement when the Stokes number decreases. This transition can be observed around the Stokes number of 1. It should be noted that the particulate loading has an effective role on the Stokes

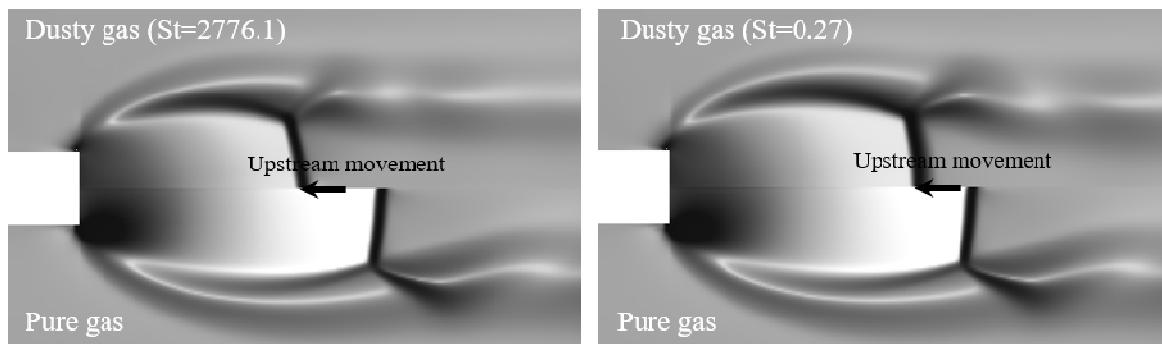


Fig. 6 Effects of addition of dust particles with different diameters on Mach disk location

number at which this transition occurs. The higher the particulate loading the more is the Mach disk displacement (either upstream or downstream). In case of $\beta = 1.07$, upstream to downstream transition is observed even for higher Stokes number ($St = 2.77$). For all the simulated test cases in Fig. 4, the streamlines of the particles overlaid on density contours of the dust phase are plotted in Fig. 5. As it can be seen from the figure, the streamlines depict an identical qualitative trend for similar Stokes number. In low Stokes number flows, dust particles can follow the gas streamlines closely; However, in higher Stokes number flows, the dust particles show a more independent movement as shown in Fig. 5. This figure can partially justify the counter-intuitive Mach disk location displacement. For the case of $St = 2776.1$ and $\beta = 1.07$, as the particles do not follow the gas phase streamline closely, a high concentration region near the jet exit can be observed. Therefore, there is a noticeable change of local particulate loading in radial direction, leading to formation of curved Mach disk as evident in Fig. 4.

3.4. Non-equilibrium effects at the exit plane

Even though numerical results confirm the downstream movement of the Mach disk, there is no experimental result which confirms this trend. Sommerfeld [18] showed the numerical solution gives a 25% over-prediction in particle velocity compared to the experimental measurements. This is partly due to consideration of rarefaction and compressibility effects in drag correlations. On the other hand, Sommerfeld [18] suggested that a reduced gas velocity equal to the equilibrium sound speed of the gas-particle mixture should be assigned at the inlet to make the simulation results closer to the experiments. In fact, presence of dust particles decelerate the gas front,

delay the gas phase expansion leading to lower exit jet velocities. While this is the actual condition in a dusty gas underexpanded jet, in our calculations we assumed that the gas obtains sonic speed at the exit. Therefore, the influence of particles inside the nozzle (before jet exit plane) is neglected. According to [18], the ratio of the equilibrium sound speed of the gas-particle mixture to the sound speed of the pure gas is given by

$$\frac{u^*}{a^*} = \sqrt{\frac{\gamma_e}{\gamma} \frac{1}{1+\beta}} \quad (22)$$

where u^* and a^* are the velocity and speed of sound at the exit plane. γ_e is the specific heat ratio of the gas-particle mixture equivalent gas. A series of simulation has been conducted in order to evaluate the level of the agreement of each approach with experimental results. The results are summarized in Table 1.

As can be observed in the table, 10 to 50% over-prediction (with a direct relationship to particulate loading) is observed. However, when the equivalent mixture speed is applied at the exit plane, the maximum deviation of the results compared to experiments is 14% for the case of $\beta = 1.08$. In Fig. 6, the Mach contours of dusty gas flow are compared with the pure gas contours. Here the equivalent mixture speed is assigned on the exit

Table 1 Comparison of the Mach disk location prediction with experimental results ($d = 26\mu\text{m}$, $St = 187.9$)

β	x_m/D	Experimental	Numerical (Sonic speed at exit plane)	Numerical (Equivalent speed at exit plane)
0.0		3.8	3.73	3.73
0.26		3.54	3.845	3.45
0.38		3.15	3.815	3.33
0.66		2.8	3.755	3.094
1.08		2.5	3.695	2.85

plane. As demonstrated in the figure, even when small particle diameters are added to the flow, the Mach disk movement is only towards upstream.

4. Conclusions

In this study, with the goal of investigation of the effects of addition of particles on the location of the Mach disk, a discontinuous Galerkin solver was applied to solve the two-fluid equation of the dusty gas flows. Despite a few limitation of the Eulerian system of equations, the method suggests advantages such as considerably lower computational costs.

The contradictory patterns of location of the Mach disk when solid particles are added into the underexpanded jet predicted in previous works was the main motivation of the current paper. Unlike the previous works which focus only on the diameter of the particles, we proposed that all the parameters which are present in the correlation of the Stokes number can affect the Mach disk location. Among these parameters the effect of variation of particle diameter and the characteristic length were investigated after the numerical tool was validated.

After demonstrating the counter-intuitive trend of the Mach disk location for different particle diameters, the effect of variation of the Stokes number independently by assigning various characteristic lengths is investigated. It was shown that the Stokes number is the main parameter which controls the mechanism of Mach disk location. For low Stokes number flows there is a downstream movement, while for high Stokes number flows there is an upstream movement. Apparently the transition in trend of Mach disk location takes place around Stokes number of 1 where the response time of the particles is in the same order of the characteristic time of the flow at the nozzle exit plane. It was shown that the effect (either upstream or downstream movement) is amplified when the particulate loading is increased.

Moreover, the deviation of the numerical results from experiments which can be modified by assigning a reduced (equilibrium speed) velocity at the exit plane of the jet was investigated. In a realistic test case (or an experimental setup) the gas and particles interact before exiting into the ambient; Therefore, the exit gas velocity is less than that of the pure gas which can substantially affect the structure of the jet. It was also shown that this consideration will lead to Mach disk locations predictions much more close to the experimental results.

Acknowledgements

This work was supported by the National Research Foundation of Korea funded by the Ministry of Science and ICT (NRF 2015-MIA3A3A02-010621), South Korea.

References

- [1] 2018, Ejtehadi, O., Rahimi, A., Karchani, A. and Myong, R.,S., "Complex Wave Patterns in Dilute Gas-Particle Flows Based on a Novel Discontinuous Galerkin Scheme," *International Journal of Multiphase Flow*, Vol.104, pp.125-151.
- [2] 1964, Carlson, D. and Lewis, C., "Normal Shock Location in Underexpanded Gas and Gas-Particle Jets," *AIAA Journal*, Vol.2, No.4, pp.776-777.
- [3] 1966, Crist, S., Glass, D. and Sherman, P., "Study of the Highly Underexpanded Sonic Jet," *AIAA Journal*, Vol.4, No.1, pp.68-71.
- [4] 1970, Avduevskii, V.S., Ivanov, A., Karpman, I.M., Traskovskii, V.D. and Yudelovich, M.Y., "Flow in Supersonic Viscous under Expanded Jet," *Fluid Dynamics*, Vol.5, No.3, pp.409-414.
- [5] 1972, Driftmyer, R.T., "A Correlation of Freejet Data," *AIAA Journal*, Vol.10, No.8, pp.1093-1095.
- [6] 1974, Antsupov, A.V., "Properties of Underexpanded and Overexpanded Supersonic Gas Jets," *Sov. Phys. Tech. Phys.*, Vol.19, No.2, pp.234-238.
- [7] 1981, Addy, A.L., "Effects of Axisymmetric Sonic Nozzle Geometry on Mach Disk Characteristics," *AIAA Journal*, Vol.19, No.1, pp.121-122.
- [8] 1987, Matsuda, T., Umeda, Y., Ishii, R. and Sawada, K., "Numerical and Experimental Studies on Choked Underexpanded Jets," *AIAA Paper 87-1378*.
- [9] 1994, Prudhomme, S.M. and Haj-Hariri, H., "Investigation of Supersonic Underexpanded Jets Using Adaptive Unstructured Finite Elements," *Finite Elements in Analysis and Design*, Vol.17, No.1, pp.21-40.
- [10] 2000, Gribben, B.J., Badcock, K.J. and Richards, B.E., "Numerical Study of Shock-Reflection Hysteresis in an Underexpanded Jet," *AIAA Journal*, Vol.38, No.2, pp.275-283.
- [11] 2008, Otobe, Y., Kashimura, H., Matsuo, S., Setoguchi, T. and Kim, H.D., "Influence of Nozzle Geometry on the near-Field Structure of a Highly Underexpanded Sonic Jet," *Journal of Fluids and*

- Structures*, Vol.24, No.2, pp.281-293.
- [12] 2015, Franquet, E., Perrier, V., Gibout, S. and Bruel, P., "Free Underexpanded Jets in a Quiescent Medium: A Review," *Progress in Aerospace Sciences*, Vol.77, pp.25-53.
- [13] 1987, Sommerfeld, M., "Expansion of a Gas/Particle Mixture in Supersonic Free Jet Flow," *Zeitschrift für Flugwissenschaften und Weltraumforschung*, Vol.11, pp.87-96.
- [14] 1988, Sommerfeld, M., "Numerical Simulation of Supersonic Two-Phase Gas-Particle Flows," *Shock Tubes and Waves*, pp.235-241.
- [15] 1988, Hayashi, A.K., Fujiwara, T., Arashi, K. and Matsuda, M., "Numerical Simulation of Gas-Solid Two-Phase Nozzle and Jet Flows," *AIAA Paper 88-2627*.
- [16] 1989, Ishii, R., Umeda, Y. and Yuhi, M., "Numerical Analysis of Gas-Particle Two-Phase Flows," *Journal of Fluid Mechanics*, Vol.203, pp.475-515.
- [17] 1967, Draper, J.S., Jarvinen, P.O., "Underexpanded Gas-Particle Jets," *AIAA Journal*, Vol.5, No.4, pp.824-825.
- [18] 1994, Sommerfeld, M., "The Structure of Particle-Laden, Underexpanded Free Jets," *Shock Waves*, Vol.3, No.4, pp.299-311.
- [19] 1993, Dobran, F., Neri, A. and Macedonio, G., "Numerical Simulation of Collapsing Volcanic Columns," *Journal of Geophysical Research: Solid Earth*, Vol.98, No.B3, pp.4231-4259.
- [20] 2007, Ongaro, T.E., Cavazzoni, C., Erbacci, G., Neri, A. and Salvetti, M.-V., "A Parallel Multiphase Flow Code for the 3d Simulation of Explosive Volcanic Eruptions," *Parallel Computing*, Vol.33, No.7, pp.541-560.
- [21] 2013, Carcano, S., Bonaventura, L., Esposti Ongaro, T. and Neri, A., "A Semi-Implicit, Second-Order-Accurate Numerical Model for Multiphase Underexpanded Volcanic Jets," *Geoscientific Model Development*, Vol.6, No.6, pp.1905-1924.
- [22] 2003, Zhang, Y. and Reese, J.M., "Continuum Modelling of Granular Particle Flow with Inelastic Inter-Particle Collisions," *Chemical Engineering Research and Design*, Vol.81, No.4, pp.483-488.
- [23] 2004, Mitter, A., Malhotra, J. and Jadeja, H., "The Two-Fluid Modelling of Gas-Particle Transport Phenomenon in Confined Systems Considering Inter Particle Collision Effects," *International Journal of Numerical Methods for Heat & Fluid Flow*, Vol.14, No.5, pp.579-605.
- [24] 2001, Zhang, Y. and Reese, J.M., "Particle-Gas Turbulence Interactions in a Kinetic Theory Approach to Granular Flows," *International Journal of Multiphase Flow*, Vol.27, No.11, pp.1945-1964.
- [25] 1994, Gidaspow, D., *Multiphase Flow and Fluidization: Continuum and Kinetic Theory Descriptions*, Academic press.
- [26] 1973, Reed, W.H. and Hill, T.R., "Triangular Mesh Methods for the Neutron Transport Equation," *Los Alamos Scientific Laboratory Technical Report LA-UR-73-479*.
- [27] 1988, Cockburn, B. and Shu, C.W., "The Runge-Kutta Local Projection P1- Discontinuous-Galerkin Finite Element Method for Scalar Conservation Laws," *RAIRO- Modélisation Mathématique et Analyse Numérique*, Vol.25, No.3, pp.337-361.
- [28] 1989, Cockburn, B. and Shu, C.W., "Tvb Runge-Kutta Local Projection Discontinuous Galerkin Finite Element Method for Conservation Laws. II. General Framework," *Mathematics of Computation*, Vol.52, No.186, pp.411-435.
- [29] 1998, Cockburn, B. and Shu, C.W., "The Runge-Kutta Discontinuous Galerkin Method for Conservation Laws V: Multidimensional Systems," *Journal of Computational Physics*, Vol.141, No.2, pp.199-224.
- [30] 2000, Cockburn, B., Karniadakis, G.E. and Shu, C.W., *The Development of Discontinuous Galerkin Methods*, Springer.
- [31] 1997, Bassi, F. and Rebay, S., "A High-Order Accurate Discontinuous Finite Element Method for the Numerical Solution of the Compressible Navier-Stokes Equations," *Journal of Computational Physics*, Vol.131, No.2, pp.267-279.